Heat-Affected-Zone Liquation Cracking in Welded Cast Haynes® 282®

metals

MDPI

Article

Heat-Affected-Zone Liquation Cracking in Welded Cast Haynes® 282®

Sukhdeep Singh [1,*] and Joel Andersson [2]

[1] Department of Industrial and Materials Science, Chalmers University of Technology, SE-41296 Gothenburg, Sweden
[2] Department of Engineering Science, University West, SE-46181 Trollhättan, Sweden; joel.andersson@hv.se
* Correspondence: sukhdeep.singh@chalmers.se; Tel.: +46-520-223-207

Received: 25 November 2019; Accepted: 13 December 2019; Published: 23 December 2019

Abstract: Varestraint weldability testing and Gleeble thermomechanical simulation of the newly developed cast form of Haynes® 282® were performed to understand how heat-affected-zone (HAZ) liquation cracking is influenced by different preweld heat treatments. In contrast to common understanding, cracking susceptibility did not improve with a higher degree of homogenization achieved at a higher heat-treatment temperature. Heat treatments with a 4 h dwell time at 1120 °C and 1160 °C exhibited low cracking sensitivity, whereas by increasing the temperature to 1190 °C, the cracking was exacerbated. Nanosecond ion mass spectrometry analysis was done to characterize B segregation at grain boundaries that the 1190 °C heat treatment indicated to be liberated from the dissolution of C–B rich precipitates.

Keywords: cracking; Varestraint; Gleeble; Haynes® 282®; nanoSIMS; boron

1. Introduction

Haynes® 282® has received considerable interest in the aerospace industry due to its improved creep strength in the temperature range of 650–930 °C, which was obtained with a lower fraction of γ′ in comparison to René 41 [1]. Besides γ′, which is the primary strengthening phase, other precipitates that have been reported in the alloy are Ti–Mo-rich MC primary carbides, Ti-rich MN nitrides, Cr-rich $M_{23}C_6$, Mo-rich M_6C secondary carbides, and Mo-rich M_5B_3 borides [1–3].

Similar to Alloy 718, which faced an early development for wrought- and later on for cast-material form, a cast Haynes® 282® has now been developed for the fabrication of aeroengine components. Early studies have investigated castability [4] and microstructural aspects [5], which reported additional precipitates such as σ and M_2SC. With regard to weldability, the wrought alloy was reported to have a good resistance to strain age cracking [1], good repair weldability [6], and lower hot-cracking susceptibility relative to Waspaloy and René 41 [2,7]. However, weldability, in terms of cracking susceptibility and its influence of preweld heat treatments, still needs to be addressed for the cast version, and is, therefore, under the scope in the present study.

Cast superalloys are generally known to perform poorly in comparison to their wrought counterparts. Poor weldability has generally been related to the higher extent of segregation that often requires preweld heat-homogenization treatments. When it comes to the wrought version of Haynes® 282®, the recommended solution heat-treatment temperature is in the range of 1120–1150 °C, which is the required temperature range for dissolving secondary carbides [8]. As for the cast version, there is no suggested available preweld heat treatment. Generally, for Fe–Ni and Ni-based superalloys, preweld temperatures are decided so that incipient melting of the low-melting Gamma-Laves eutectic is avoided, which occurs in the range of 1150–1160 °C. This is generally carried out by two different hot isostatic pressing (HIP) approaches, commonly employed in the aerospace industry,

at 1120 °C and 1190 °C [9–11], respectively, below and above the melting of the Laves eutectic. The aforementioned preweld heat treatment temperatures were investigated for the cast Alloy 718 [12] and ATI® 718Plus™ [13]. Even though Haynes® 282® is devoid of detrimental Laves phases, a common heat treatment for the three superalloys that minimizes cracking is interesting from an industrial perspective. In the current investigation, pseudo-HIP treatments were performed in a small laboratory furnace without any pressure effects. Besides solution temperatures of 1120 °C and 1190 °C, an additional temperature of 1160 °C was used in the present study. The objective was, therefore, to investigate how the material behaves in respect to heat-affected-zone (HAZ) liquation-cracking susceptibility after being subjected to the aforementioned heat treatments.

2. Materials and Methods

The composition of the material used in this study is presented in Table 1. Cast plates were heat treated at temperatures of 1120 °C, 1160 °C, and 1190 °C for 4 h of dwell time, followed by solution heat treatment at 1135 °C for 30 min and quenched in water.

Table 1. Chemical composition of cast Haynes® 282® in wt. % provided by material supplier.

Ni	Cr	Fe	Co	Nb	Mo	Al	Ti	C	W	Mn	Cu	Si	P	B	Ta	S
Bal.	19.3	0.2	9.9	0.1	8.5	1.44	2.07	0.05	0.1	0.1	0.1	0.01	0.004	0.006	0.1	0.001

Test plates were cut out to the final dimensions of 150 mm × 60 mm × 3.3 mm for Varestraint testing. State-of-the-art Varestraint weldability testing [14] based on the original test developed by Savage and Lundin [15] was used. The test setup is shown in Figure 1.

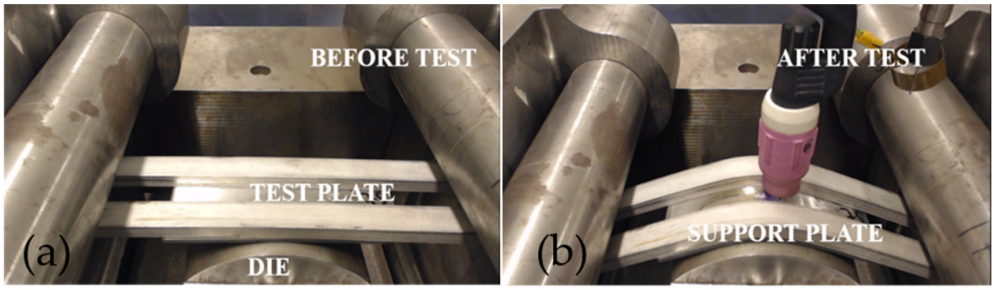

Figure 1. Varestraint testing setup (**a**) before and (**b**) after test.

Welding and testing parameters, which are based on experiment design that produced the lowest standard deviation for crack measurements among different settings [14], are summarized in Table 2. Longitudinal Varestraint weldability testing was performed at 3 strain levels of 1.1%, 1.6%, and 2.7% augmented strain. Three test plates were tested for each condition and strain level.

Table 2. Parameters for Varestraint weldability testing using tungsten gas arc welding.

Welding Speed (mm/s)	Stroke Rate (mm/s)	Welding Current (A)	Arc Length (mm)	Argon Gas Flow (l/min)
1	10	70	2	15

After Varestraint weldability testing, the oxide layer was manually removed by the use of fine abrasive paper. Crack measurements were performed using a stereomicroscope at magnifications of 20–50 times. Gleeble 3800D thermomechanical testing was used to physically simulate the HAZ during welding. Tests were performed by rapid heating at 111 °C/s to 3 test temperatures of 1050 °C, 1150 °C, and 1200 °C, with a holding time of 0.03 s. Samples then were pulled to fracture at a stroke rate of 55 mm/s. Cross sections from the base metal and HAZ were cut, mounted, and polished

with 9 and 3 µm discs. Macroetching with a solution of 90% HCl and 10% HNO_3 was used for grain-size measurement, whereas samples were etched electrolytically by oxalic acid at 3.2 V for microstructure evaluation by light optical microscopy (LOM) and scanning electron microscopy (SEM) LEO 1550 FEG-SEM (LEO GmbH, Oberkoche, Germany) equipped with Oxford electron dispersive X-ray spectroscopy. Grain-size measurements and volume fraction of secondary precipitates were measured according to the ASTM (American Society for Testing and Materials) E112-96 [16] and E562-08 [17] standards, respectively. Macrohardness Vickers test (HV10) was done on 3 test samples for each material condition. Grain-boundary segregation was examined by a CAMECA NanoSIMS 50L secondary ion mass spectrometer (CAMECA, Gennevilliers, France) using a primary beam of Cs^+. Mass-resolved images were obtained for $^{11}B^-$, $^{12}C_2{}^-$, $^{28}Si^-$, $^{31}P^-$, and $^{11}B^{16}O_2{}^-$. JMatPro v8 (version 8, Sente Software, Surrey, UK) was used for phase prediction.

3. Results & Discussion

3.1. Microstructure

The base-metal microstructure through LOM can be seen in Figure 2. High-magnification SEM images show the homogenization effect along the grain boundaries of the initial as-cast condition (Figure 3a) and at 1190 °C/4 h (Figure 3b).

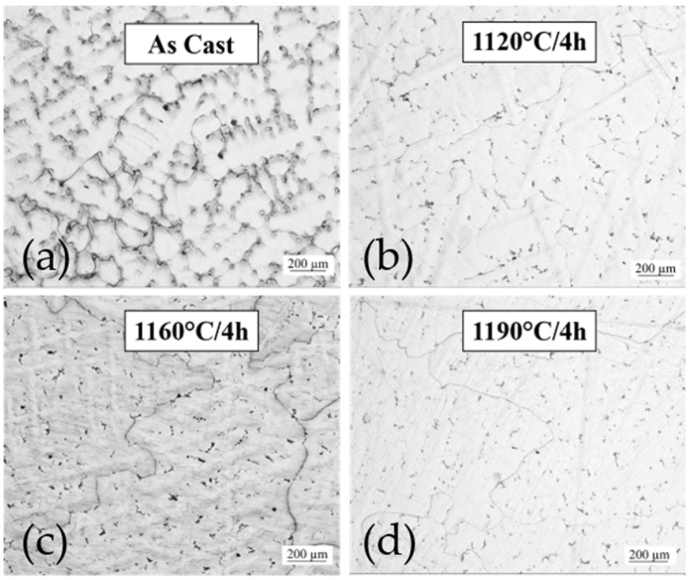

Figure 2. Optical images showing base-metal segregation extent in four conditions: (**a**) As cast, and at (**b**) 1120 °C/4 h, (**c**) 1160 °C/4 h, and (**d**) 1190 °C/4 h.

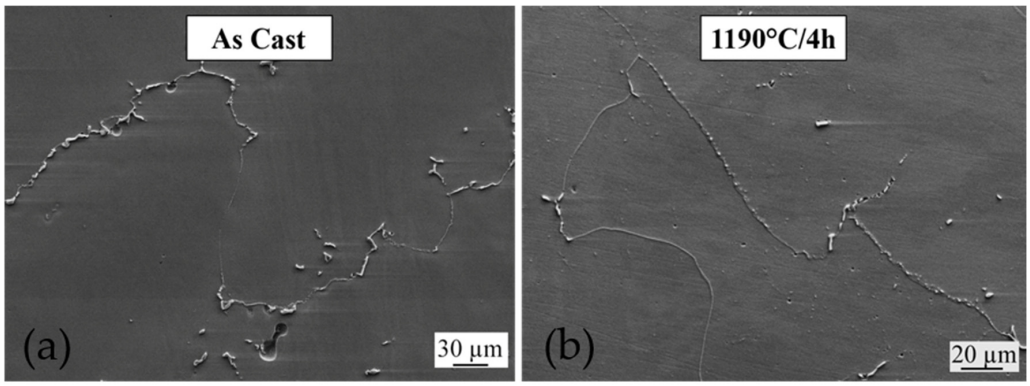

Figure 3. Scanning electron microscopy (SEM) images showing homogenization effect along grain boundaries (**a**) as cast and at (**b**) 1190 °C/4 h.

Segregation was reduced by increasing heat-treatment temperature both in the matrix and along the grain boundaries. The quantification of secondary precipitates in terms of volume fraction (Vv%) showed the highest value in the as-cast condition of about 1.5% and decreased with increasing heat-treatment temperature to about 0.5% after heat treatment at 1190 °C (Figure 4).

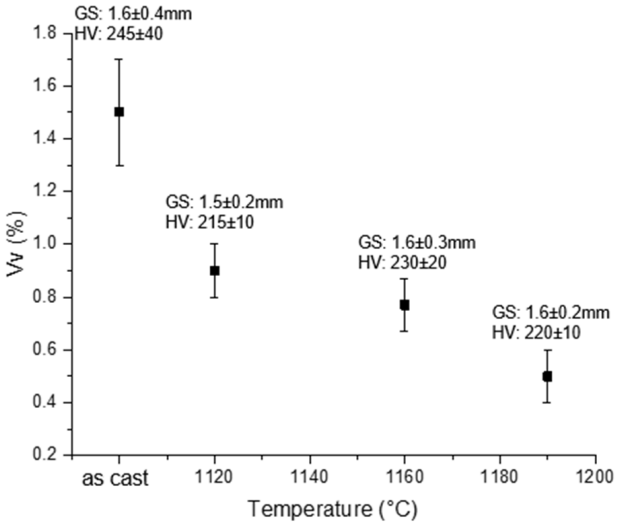

Figure 4. Volume fraction of secondary phases, hardness, and grain size values for the different conditions.

A magnified image of the interdendritic region of the 1120 °C heat-treatment condition shows the presence of large MC carbides and small Mo-rich precipitates (Figure 5).

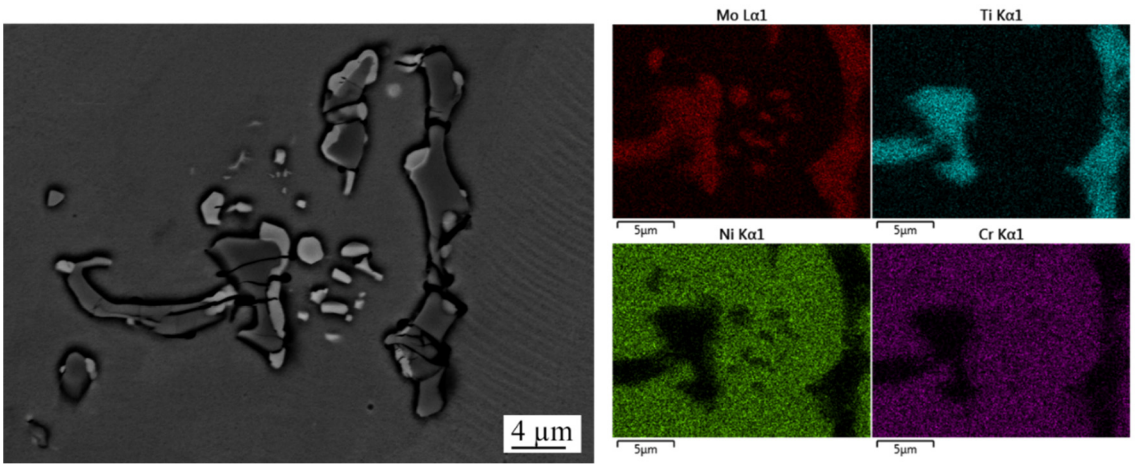

Figure 5. SEM energy-dispersive X-ray spectroscopy (EDS) maps showing segregation of Ti–Mo-rich carbides and Mo-rich precipitates in interdendritic areas after heat treatment at 1120 °C/4 h.

At 1160 °C/4 h, Mo-rich precipitates were still present, but to a lower extent, whereas 1190 °C/4 h was able to dissolve them, and only MC carbides were present (Figure 6).

Base-metal hardness did not experience significant change after heat treatment, with hardness level in the range of 215–230 HV in the heat-treated conditions, and about 245 HV in the as-cast condition (Figure 4). The average grain size of about 1.6 mm remained similar after all three heat treatments.

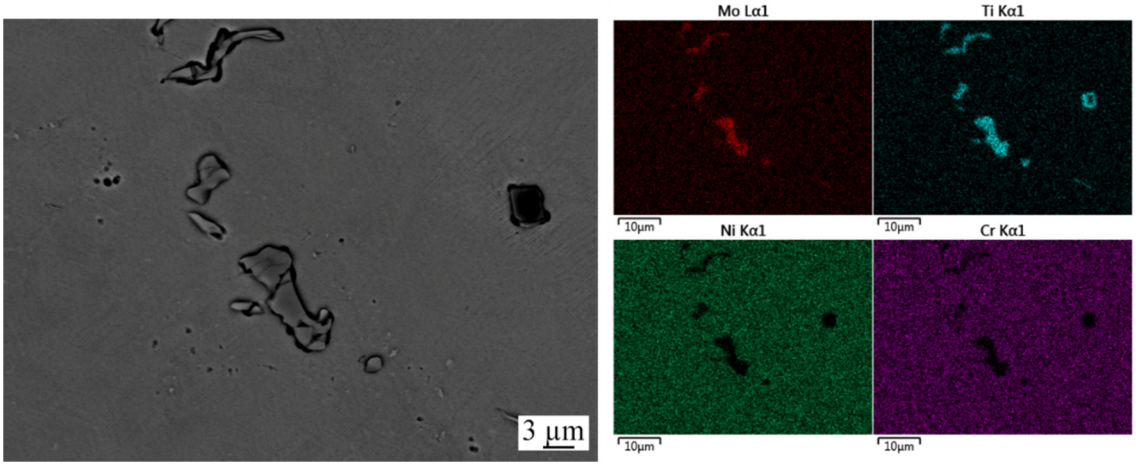

Figure 6. SEM-EDS maps showing segregation of Ti–Mo-rich carbides after heat treatment at 1190 °C/4 h.

3.2. Varestraint Testing

The results from HAZ crack measurements are plotted in Figure 7. Despite the large scatter, which is typical in testing of cast materials, as reported in previous studies [11,12], it can be seen that cracking-behavior results are similar for the preweld heat treatments at 1120 °C and 1160 °C, which exhibited the least amount of cracking, whereas the 1190 °C heat-treatment condition exhibited the highest amount of cracking.

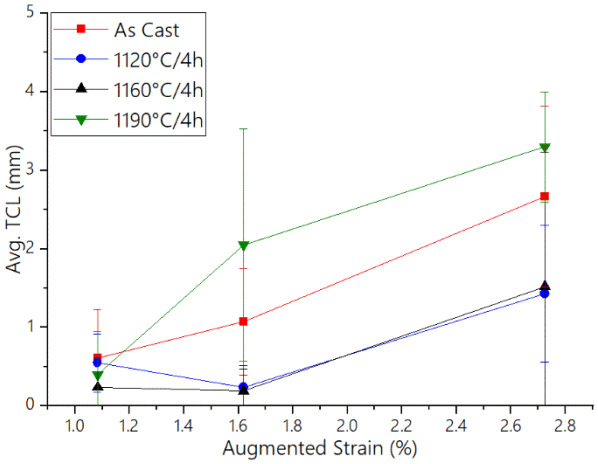

Figure 7. Average total crack length (TCL) in heat-affected zone (HAZ).

Cracking occurred both in fusion and HAZ, but cracking susceptibility in the fusion zone (FZ) did not reveal any difference between the different conditions. The results and discussion are, therefore, only related to HAZ liquation cracking. At first, after being subjected to the preweld heat treatment at 1120 °C and 1160 °C, respectively, HAZ cracking susceptibility of Haynes® 282® decreased. However, increasing the heat-treatment temperature to 1190 °C had an adverse effect, since cracking susceptibility increased further. Many studies related cracking susceptibility as a function of the homogenization extent. In general, the more homogenization, the less cracking, as the amount of secondary precipitates contributing to liquation were also reduced [18]. In the current study, however, the homogenization heat treatment at 1190 °C, with about 0.5 Vv% of secondary precipitates, was seen to exhibit the most detrimental behavior in relation to HAZ cracking. Other factors, such as hardness, which is a parameter used to indicate the stress-relaxation properties of the material, and grain size, do not explain the cracking trend between the tested conditions, as their values were almost the same. HAZ cracks formed along the grain boundaries, horizontally to the fusion line, and they were absent of the eutectic

constituents commonly seen in other Fe–Ni and Ni-based superalloys. However, cracks were often seen to be connected to the FZ, having traces of backfilled liquid, as can be seen in Figure 8.

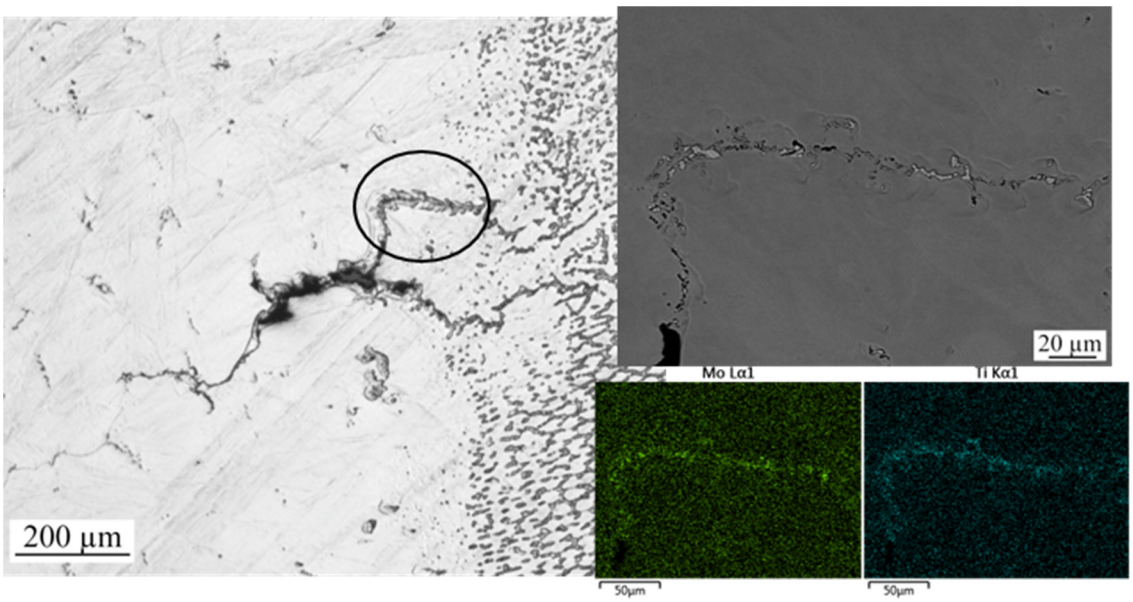

Figure 8. HAZ liquation cracking showing crack with backfilled liquid from fusion zone enriched in Mo and Ti.

3.3. Gleeble Thermomechanical Simulation

Gleeble thermomechanical simulation was used to investigate HAZ grain-boundary properties by isolating the effect from the FZ. The HAZ thermal cycle of preweld samples, heat treated at 1120 °C and 1190 °C, respectively, was performed by rapidly heating to three different peak temperatures below the equilibrium solidus of the alloy and pulled to fracture to measure on-heating ductility response. On-heating ductility profiles are plotted with reference values for wrought Haynes® 282® [19] in Figure 9.

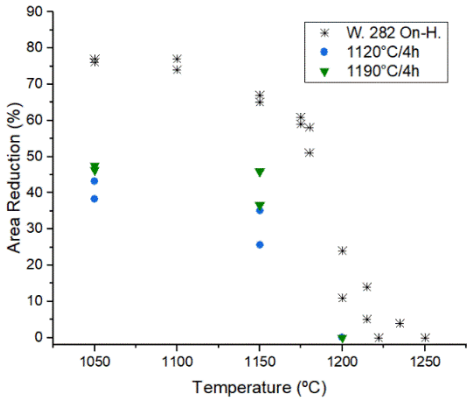

Figure 9. Gleeble on-heating ductility for cast and wrought Haynes® 282®, data from [19].

Figure 9 shows that the area-reduction values for 1120 °C were slightly lower than for 1190 °C, with a ductility drop starting at about 1150 °C and approaching 0% at 1200 °C. The ductility drop is generally attributed to the formation of a liquid phase that was responsible for the embrittlement of the grain boundaries. The microstructure in the test samples at 1150 °C appeared to be unaffected in both heat treatments. When looking at fracture surfaces, the fracture occurred in a ductile manner with a characteristic dimpled surface (Figure 10). However, at high magnification, the fracture-surface area revealed roundish features, indicating that liquid was present at 1150 °C [20]. This suggests that

the fracture occurred in a combined ductile–brittle mode. Only MC carbides were seen to liquate at 1200 °C in the 1190 °C heat-treatment condition, whereas extensive liquation of MC carbides and secondary phases had occurred at grain boundaries in the 1120 °C heat-treatment condition (Figure 11).

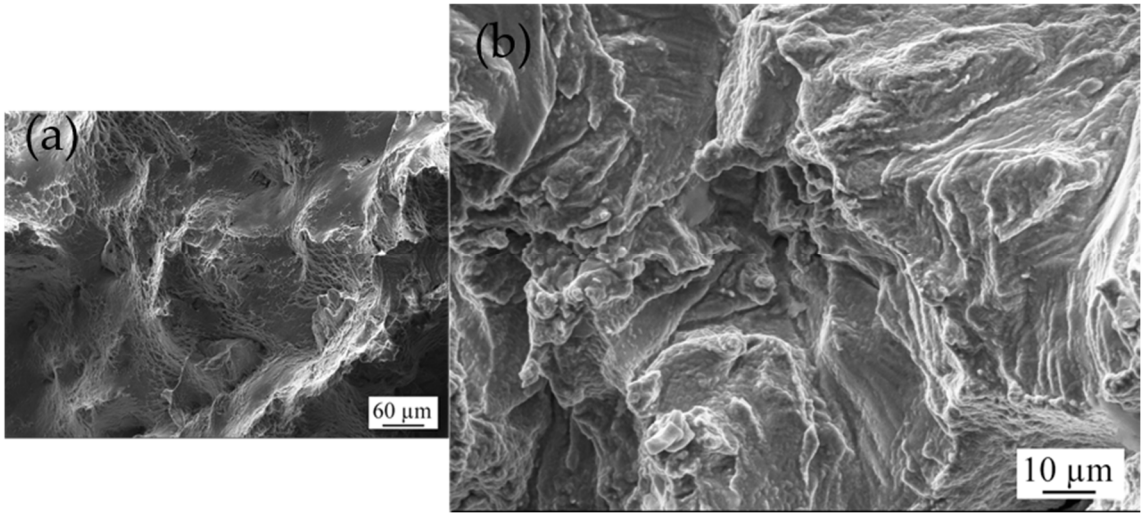

Figure 10. Fracture surface of 1190 °C heat-treatment condition tested at 1150 °C. (**a**) Typical dimples occurring in ductile fracture, (**b**) higher magnification showing traces of liquation covering fracture surface with small round features.

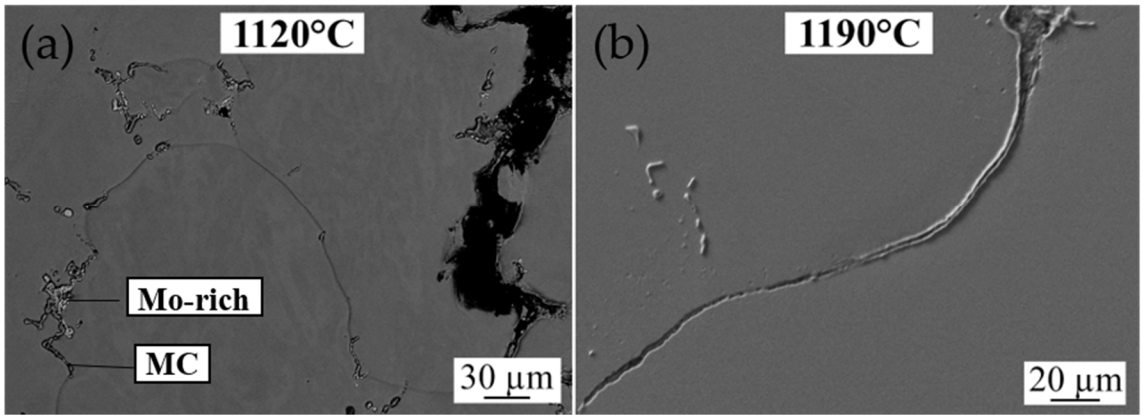

Figure 11. SEM images showing extent of liquation at (**a**) 1120 °C/4 h and (**b**) 1120 °C/4 h after Gleeble testing at 1200 °C.

As test temperatures were well below the alloy equilibrium solidus of 1244 °C [3], the formation of the liquid phase could be attributed to subsolidus melting that can occur by a liquation mechanism, or when the melting point is locally suppressed by low melting phases or elements. As Haynes® 282® does not seemingly have a low melting temperature phase, it is likely that segregation of minor elements at grain boundaries was responsible for lowering the melting temperature.

It is interesting to see that the 1190 °C condition, which exhibited enhanced cracking, also showed rather high on-heating ductility. Correlation of the Varestraint and Gleeble results is often used for analyzing similar trends, but the hot ductility test is used to assess the tendency of the material to liquate. It has been reported that the test is sensitive to liquation reaction temperatures and a temperature range over which liquid is present; however, this does not indicate any difference in the extent of, e.g., grain-boundary wetting [21].

3.4. NanoSIMS

The presence of minor elements at the grain boundaries was investigated by nanoSIMS. The elements included in the analysis were C, B, Si, and P. However, no Si and P were detected. Analysis revealed B-rich discrete precipitates in the 1120 °C/4 h condition, as visible in Figure 12. These precipitates were in association with C-rich particles.

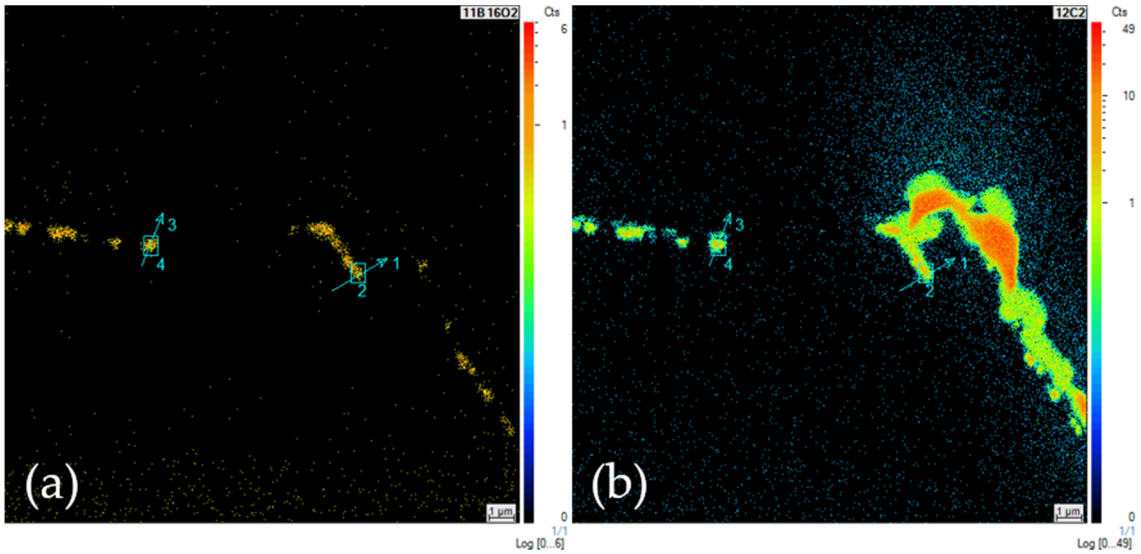

Figure 12. Elemental map showing particle segregation of (**a**) B and (**b**) C along grain boundary in 1120 °C/4 h condition.

Similarly, B was also entrapped in the form of particles in the 1160 °C/4 h condition (Figure 13).

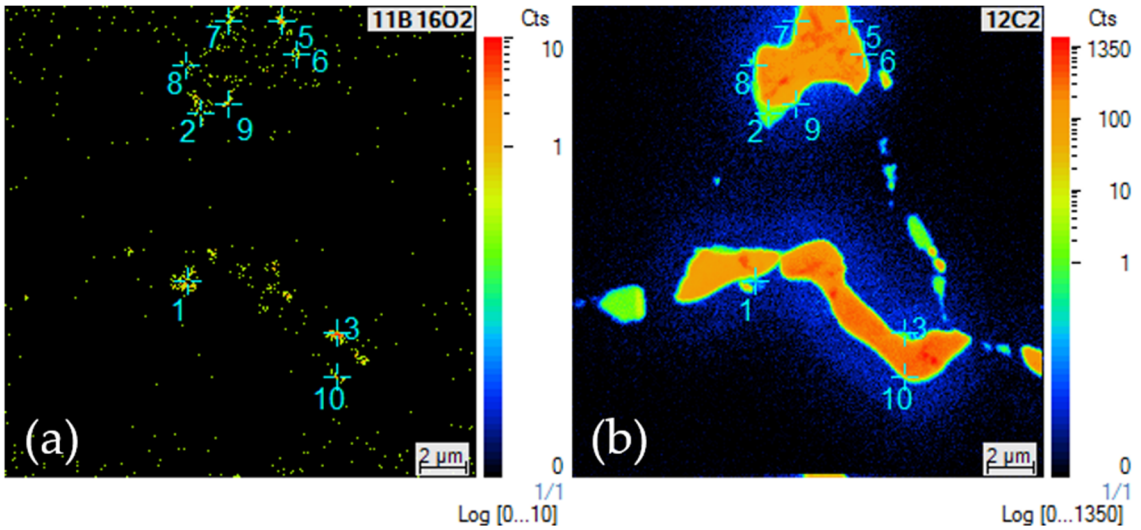

Figure 13. Elemental map showing (**a**) B segregation at interface of (**b**) Ti–Mo (MC) carbides at 1160 °C.

At 1190 °C, B was found to be present in free form at the grain boundaries (Figure 14). This temperature was high enough to dissolve the B-rich particles. Line scans clearly revealed that B was segregated at the grain boundaries.

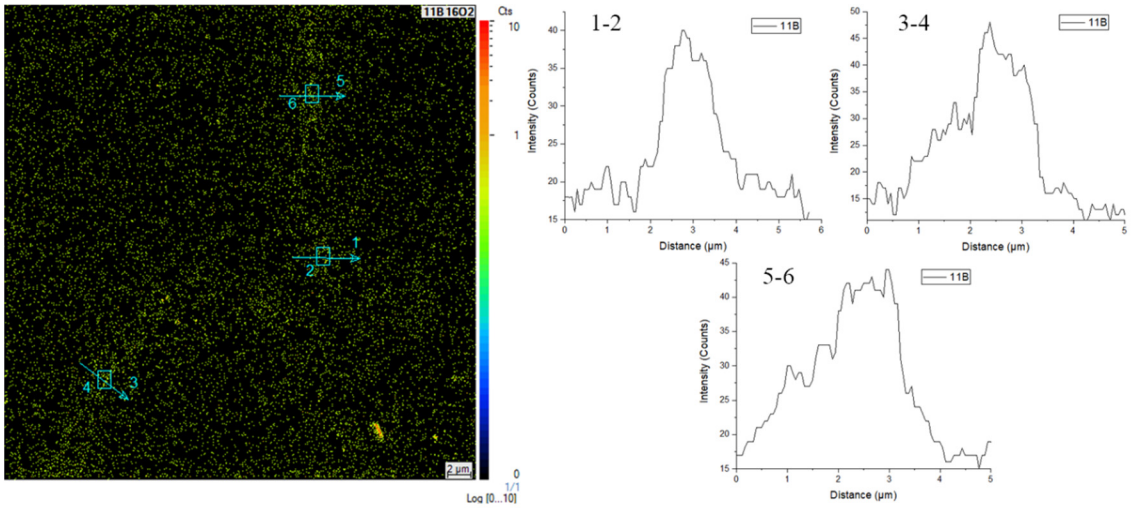

Figure 14. Elemental map and line scans showing B enrichment along grain boundaries in 1190 °C/4 h condition.

To the authors´ best knowledge, B segregation has not been previously reported in the cast Haynes® 282®. B has been reported to segregate in steels and superalloys according to the nonequilibrium segregation mechanism [22–24]. The tendency of segregation is known to increase with increasing heat-treatment temperature, but is also highly dependent on the cooling rate after heating. Free B was not present at the heat-treatment temperatures of 1120 °C and 1160 °C, meaning that nonequilibrium segregation was not effective at these temperatures. At 1190 °C/4 h, the decomposition of C–B precipitates allowed B to diffuse and segregate at the boundaries.

JMatPro simulation results from Figure 15 suggested that the B-rich phases could have been M_3B_2. However, M_3B_2 has rarely been reported in superalloys [5]. It is possible that these are M_5B_3, as reported by Osoba et al. [3] in wrought Haynes® 282®. Nevertheless, B is known to have a detrimental effect on weldability. In a study by Caron [2] investigating the weldability of wrought Haynes® 282®, varying B content, from 30 to 50 ppm, led to an increasing amount of cracking, from about 1 to 2.5 mm in total crack length (TCL). Similarly, Osoba et al. [3] found that the preweld heat treatment that favored the most severe effect on B segregation also exacerbated cracking.

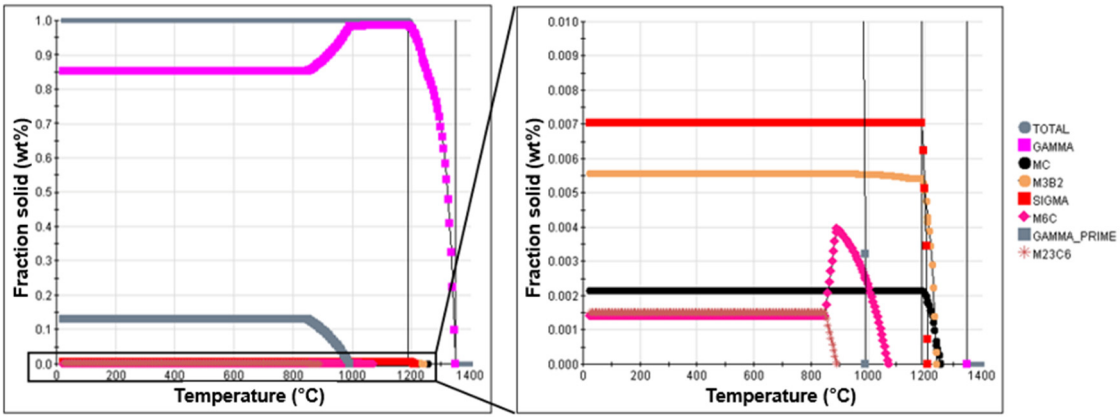

Figure 15. JMatPro simulation predicting precipitates forming in Haynes® 282®.

Therefore, exacerbated cracking in the 1190 °C condition seemed to be related to B segregation from the dissolution of C–B-rich precipitates at the grain boundaries, which is known to suppress the local liquation starting temperature, thereby enlarging the effective melting range of the alloy. Subsolidus melting is not the only effective mechanism for HAZ cracking; besides being a potent melting-point depressant, B is also a surface active element that improves the wetting property of

the liquid so that the liquid is present in continuous form [21,25]. As clearly visible from Figure 11, the extent of the liquid phase at the grain boundaries was higher at 1120 °C/4 h, characterized by relatively large but disconnected melted areas. On the other hand, at 1190 °C/4 h, no liquated products could be seen, meaning that little amount of liquid was available. Thin and continuous liquid films are reported to be more damaging from a cracking perspective relative to when they are present in a thick and disconnected form [26].

4. Conclusions

The following were concluded from the present study:

- Heat treatments at 1120 and 1160 °C/4 h had similar HAZ cracking susceptibility in Varestraint testing, whereas heat treatment at 1190 °C/4 h had the most detrimental cracking behavior;
- On-heating Gleeble hot ductility tests indicated that subsolidus melting starts at ~1150 °C, which is a significantly lower temperature than that of the equilibrium solidus for the alloy.
- B-rich precipitates, possibly carboborides, were found in the conditions of 1120 and 1160 °C/4 h, whereas heat treatment at 1190 °C/4 h completely dissolved the carboborides, which led to B atoms being released from the dissolution of these precipitates and segregated to the grain boundaries;
- The complete dissolution of C–B particles and the segregation of B at the grain boundaries at 1190 °C exacerbated HAZ cracking;

Author Contributions: Conceptualization, S.S. and J.A.; Methodology, S.S. and J.A.; Investigation, S.S.; Supervision, J.A.; Writing—original draft, S.S.; Writing—review & editing, J.A.; Funding acquisition, J.A. All authors have read and agreed to the published version of the manuscript.

Funding: The authors highly appreciate the financial support from SpaceLAB through European Regional Development Fund and GKN (Guest, Keen and Nettlefolds) Aerospace Sweden AB.

Acknowledgments: The authors would like to thank Tahira Raza at University West for help with Varestraint testing; Aurélien Thomen for his help on measurement acquisition performed on the NanoSIMS facility at the Chemical Imaging Infrastructure, Chalmers University of Technology and University of Gothenburg, supported by the Knut and Alice Wallenberg Foundation; and Professor Olanrewaju Ojo at the University of Manitoba for the valuable input and discussions.

Conflicts of Interest: The authors declare no conflict of interest.

References

1. Pike, L.M. Development of a fabricable gamma-prime (γ′) strengthened superalloy. *Superalloy* **2008**, *2008*, 191–200.
2. Caron, J. Weldability and Welding Metallurgy of Haynes 282 Alloy. In *Proceedings of the 8th International Symposium on Superalloy 718 and Derivatives*; John Wiley & Sons: Pittsburg, CA, USA, 2014; p. 273.
3. Osoba, L.O.; Ding, R.G.; Ojo, O.A. Improved Resistance to Laser Weld Heat-Affected Zone Microfissuring in a Newly Developed Superalloy HAYNES 282. *Metall. Mater. Trans. A* **2012**, *43*, 4281–4295. [CrossRef]
4. Sobczak, N.; Pirowski, Z.; Purgert, R.M.; Uhl, W.; Jaskowiec, K.; Sobczak, J.J. Castability of HAYNES 282 alloy. In Proceedings of the Workshop "Advanced Ultrasupercritical Coal-Fired Power Plants", Vienna, Austria, 19–20 September 2012; pp. 19–20.
5. Matysiak, H.; Zagorska, M.; Andersson, J.; Balkowiec, A.; Cygan, R.; Rasinski, M.; Pisarek, M.; Andrzejczuk, M.; Kubiak, K.; Kurzydlowski, K. Microstructure of Haynes 282 Superalloy after Vacuum Induction Melting and Investment Casting of Thin-Walled Components. *Materials* **2013**, *6*, 5016–5037. [CrossRef] [PubMed]
6. Hanning, F.; Andersson, J. Weldability of wrought Haynes 282 repair welded using manual gas tungsten arc welding. *Weld. World* **2018**, *62*, 39–45. [CrossRef]
7. Jacobsson, J.; Andersson, J.; Brederholm, A.; Hanninen, H. Weldability of Ni-Based Superalloys Waspaloy and Haynes 282—A Study Performed with Varestraint Testing. *Res. Rev. J. Mater. Sci.* **2016**, *4*, 3–11.
8. Singh, S. Precipitation of Carbides in a Ni-based Superalloy. Master's Thesis, University West, Trollhättan, Sweden, 2014.

9. Barron, M.L. *Crack Growth-Based Predictive Methodology for the Maintenance of the Structural Integrity of Repaired and Nonrepaired Aging Engine Stationary Components*; GE Aircraft Engines: Cincinnati, OH, USA, 1999.
10. Snyder, S.M.; Brown, E.E. Laves Free Cast + Hip Nickel Base Superalloy. U.S. Patent No 4,750,944, 1988.
11. Paulonis, D.F.; Schirra, J.J. Alloy 718 at Pratt and Whitney—Historical perspective and future challenges. *Superalloys* **2001**, *718*, 13–23.
12. Singh, S.; Andersson, J. Hot cracking in cast alloy 718. *Sci. Technol. Weld. Join.* **2018**, 568–574. [CrossRef]
13. Singh, S.; Andersson, J. Varestraint weldability testing of cast ATI 718Plus—A comparison to cast Alloy 718. *Weld. World* **2019**, *63*, 389–399. [CrossRef]
14. Andersson, J.; Jacobsson, J.; Lundin, C. A Historical Perspective on Varestraint Testing and the Importance of Testing Parameters. In *Cracking Phenomena in Welds IV*; Springer: Berlin/Heidelberg, Germany, 2016; pp. 3–23.
15. Savage, W.F.; Lundin, C.D. The Varestraint Test. *Weld. J.* **1965**, 433–442.
16. *Standard Test Methods for Determining Average Grain Size*; ASTM Int.: West Conshohocken, PA, USA, 2004; pp. E112–E196.
17. *Standard Test Method for Determining Volume Fraction by Systematic Manual Point Count*; ASTM Int.: West Conshohocken, PA, USA, 2008; pp. E508–E562.
18. Singh, S. Varestraint Weldability Testing of Cast Superalloys. Ph.D. Thesis, Chalmers University of Technology, Göteborg, Sweden, 2018.
19. Andersson, J.; Chaturvedi, M.; Sjörberg, G. Hot Ductility Study of HAYNES 282 Superalloy. In Proceedings of the 7th International Symposium on Superalloy 718 and Derivatives, Pittsubrgh, PA, USA, 10–13 October 2010; Volume 718, pp. 539–554.
20. Qian, M. An Investigation of the Repair Weldability of Waspaloy and Alloy 718. Ph.D. Thesis, The Ohio State University, Columbus, OH, USA, 2001.
21. West, S.L. A Study of Weld Heat-Affected Zone Liquation Cracking in Cast Nickel-Base Superalloys. Ph.D. Thesis, The Ohio State University, Columbus, OH, USA, 1991.
22. Karlsson, L.; Norden, H. Grain boundary segregation of boron. An experimental and theoretical study. *J. Phys. Colloq.* **1986**, *47*, 257–262. [CrossRef]
23. Karlsson, L.; Nordén, H.; Odelius, H. Overview no. 63 Non-equilibrium grain boundary segregation of boron in austenitic stainless steel—I. Large scale segregation behaviour. *Acta Metall.* **1988**, *36*, 1–12. [CrossRef]
24. Huang, X.; Chaturvedi, M.C.; Richards, N.L. Effect of homogenization heat treatment on the microstructure and heat-affected zone microfissuring in welded cast alloy 718. *Metall. Mater. Trans. A* **1996**, *27*, 785–790. [CrossRef]
25. Kelly, T.J. Elemental effects on cast 718 weldability. *Weld. J.* **1989**, *68*, 44–51.
26. Owczarski, W.A.; Duvall, D.S.; Sullivan, C.P. A model for heat affected zone cracking in nickel-base superalloys. *Weld. J.* **1966**, *45*, 145.